Synthesis and chiroptical properties of hexa-, octa- and deca-azaborahelicenes: influence of the helicene's size and of the number of boron atoms

Chengshuo Shen,[a] Monika Srebro-Hooper,*,[b] Marion Jean,[c] Nicolas Vanthuyne,[c] Loïc Toupet,[a] J. A. Gareth Williams,[d] Alexis R. Torres,[e] Adrian J. Riives,[e] Gilles Muller,[e] Jochen Autschbach,*,[f] and Jeanne Crassous*,[a]

Dedication ((optional))

Abstract: Four members of a new class of cycloborylated hexa- to deca-helicenes (**1a**-**d**) have been prepared in enantiopure forms, along with cycloplatinated deca-helicenes (**1d'**, **1d**^{1}) further extending a family of cycloplatinated hexa- to octa-helicenes reported previously. The azabora[*n*]helicenes display intense electronic circular dichroism and strong optical rotations, whose dependence on the size of the helix (*n* = 6, 8, or 10) and number of boron atoms (1 or 2) has been examined in detail both experimentally and theoretically. The photophysical properties (unpolarized and circularly polarized luminescence) of these new fluorescent organic helicenes have been measured and compared with the corresponding organometallic phosphorescent cycloplatinated derivatives (**1a**^{1}-**d**^{1}).

Introduction

Heteroatomic polycyclic aromatic hydrocarbons (heteroatomic PAHs) are attractive due to their potential use as materials for organic electronics such as organic light-emitting diodes (OLEDs), organic field-effect transistors (OFETs), or organic photovoltaics (OPVs).[1] Representative achiral heteroarenes are, for instance, graphene analogues doped with heteroatoms (Si, S, B, N, P).[2] Heterohelicenes, on the other hand, may be considered as chiral heteroatomic PAHs.[3] Within this class of molecules, borahelicenes and azaborahelicenes have revealed strong emission (non-polarized and circularly polarized) properties[4a,b] and interesting carrier-transport abilities.[4c,d] In these molecular systems, the C=C units are replaced by isoelectronic B=C or B=N moieties, which represent two attractive means of modifying the electronic properties of achiral and chiral PAHs without changing their molecular size.[5] Aside from the 3-coordinate boron derivatives, extended π-conjugated molecules incorporating 4-coordinate boron groups are also under current development and have demonstrated potential applications in OLEDs, OFETs, photoresponsive materials, sensors and imaging materials.[6] For instance, Wang and co-workers synthesized a series of boron complexes bearing phenyl-pyridine-type C^N chelates which display a reversible photo-thermal color switching.[7a-c] A similar type of compound has been recently used for two-photon absorption and fluorescence microscopy.[7d] However, to our knowledge similar *chiral* 4-coordinate boron derivatives based on helicenes are still not known.

In this paper, we report the synthesis of azabora[*n*]helicenes of different size (from *n* = 6 up to 10 *ortho*-fused cycles) bearing one or two 4-coordinate boron atoms (**1a**-**d** in Figure 1). Strong chiroptical properties, blue fluorescence and circularly polarized luminescence (CPL) of these readily prepared novel heterohelicenes are examined and analyzed with the help of quantum-chemical calculations in terms of the size of the helicene and number of heteroatoms, and compared with previously described platina[*n*]helicenes (**1a**^{1}-**c**^{1}, Figure 1),[8a,b,e,f] as well as the novel bis-platina[10]helicene **1d**^{1}.

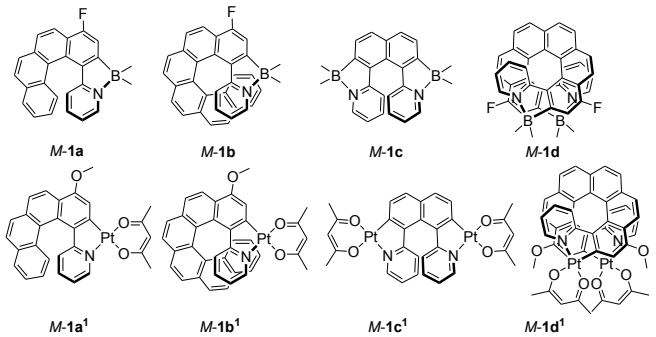

Figure 1. Chemical structures of the azaborahelicenes studied and of their corresponding platina[*n*]helicenes analogues.

Results and Discussion

Synthesis and characterization of mono- and bis-azabora[*n*]helicenes (*n* = 6, 8, 10) and bis-platina[10]helicene

In 2010, our group reported the first helicenes incorporating a metal ion into the helical backbones, named

[a] Institut des Sciences Chimiques de Rennes, UMR 6226, Institut de Physique de Rennes, UMR 6251, Campus de Beaulieu, CNRS-Université de Rennes 1, 35042 Rennes Cedex, France. E-mail: jeanne.crassous@univ-rennes1.fr
[b] Faculty of Chemistry, Jagiellonian University, R. Ingardena 3, 30-060 Krakow, Poland. E-mail: srebro@chemia.uj.edu.pl
[c] Aix Marseille University, CNRS, Centrale Marseille, iSm2, Marseille, France.
[d] Department of Chemistry, University of Durham, Durham, DH1 3LE, UK.
[e] Department of Chemistry, San José State University, San José, CA 95192-0101, USA.
[f] Department of Chemistry, University at Buffalo, State University of New York, Buffalo, NY 14260, USA. E-mail: jochena@buffalo.edu

Supplementary information for this article is given via a link at the end of the document.

metallahelicenes.[8] For instance, we developed a straightforward strategy for the synthesis of platina[6]helicenes, from a benzophenanthrene substituted with a 2-pyridyl. This *ortho*-fused π-conjugated phenyl-pyridine type ligand underwent a cycloplatination with a platinum source such as K_2PtCl_4 or $Pt(dmso)_2Cl_2$ followed by a reaction with sodium acetylacetonate (Scheme 1a).[8a-c] This synthetic strategy was generalized to the larger cycloplatinated hepta- and octa-helicenes,[8e] and extended to other metal ions, such as iridium[8a] or osmium.[8g] Herein, we describe the extension of the approach to include heteroatoms such as boron in the helicene structures.

Murakami *et al*. have recently reported a simple synthesis[9a] for azaborole derivatives in a two-step process starting from 2-phenylpyridine. First, a cycloborylation reaction of 2-phenylpyridine with BBr_3 in the presence of $N(^iPr)_2Et$ affords a *B*,*B*-dibromo-azaborole system, which then can react with AlR_3, where the bromine atoms are replaced by alkyl groups to form a *B*,*B*-dialkyl-azaborole derivative (Scheme 1b). The method takes advantage of the nitrogen atom which directs the electrophilic aromatic borylation to the *ortho*-position. Interestingly, such dialkyl-azaborole derivatives display blue fluorescence both in solid and in solution states, with high quantum yields.[9b-d]

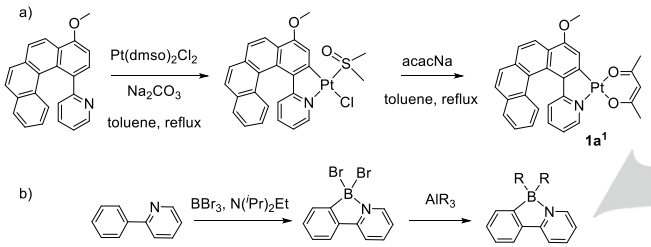

Scheme 1. a) Synthesis of platina[6]helicene **1a**[1]. b) General synthetic route to the azaborole derivative studied here.

Following a similar synthetic route, we obtained a series of azaborahelicenes containing different numbers of fused cycles in a helicene backbone and different numbers of boron atoms, namely azabora[6]helicene **1a**, azabora[8]helicene **1b**, bis-azabora[6]helicene **1c**, and bis-azabora[10]helicene **1d** (Figure 1 and Scheme 2).

The racemic azabora[6]helicene **1a** was prepared in a two-step reaction from previously described 1-fluoro-4-(2-pyridyl)-benzo[g]phenanthrene **2a**.[8a] The fluoro substituent has a protective role, enforcing regioselective photocyclization during the preparation of **2a** (see ref. [8a]). Furthermore, contrary to the methoxy group, commonly used in the platina[*n*]helicene series, the fluorine is inert to the borylation conditions. Using the procedure depicted in Scheme 2, racemic compound (±)-**1a** was thus obtained in 89% overall yield and then fully characterized (see Supplementary Information, SI). For example, the ^1H NMR shows a doublet at 7.64 ppm corresponding to the proton H^3 ($^3J_{HF}$ = 8.9 Hz), and two signals at 0.09 and 0.37 ppm for the methyl groups that are diastereotopic due to the presence of the helicene. The ^{11}B NMR displays one broad signal at 0.3 ppm and the ^{19}F NMR shows a doublet at −120.4 ppm, ($^3J_{HF}$ = 8.9 Hz, coupling with H^3).

Similarly, racemic azabora[8]helicene **1b** was synthesized from the racemic ligand **2b** which corresponds to the [6]helicene substituted at position 1 by a 2-pyridyl group (Scheme 2). **2b** was prepared as described in Scheme 3. A Wittig reaction starting from the benzo[c]phenanthrylmethyl-phosphonium bromide **3b**[10] and 2-fluoro-5-(pyridine-2-yl)benzaldehyde **4b**[8a] yielded stilbene derivative **5b** in 92% yield. Then a photocyclization reaction in a highly diluted toluene solution under irradiation for 16 hours using a mercury lamp with *in situ* oxidation (using catalytic amounts of iodine under air) generated the target racemic ligand **2b** in 56% yield. Note that **2b** corresponds to a functionalized carbo[6]helicene; it is therefore configurationally stable and exists as a racemic mixture of both *P* and *M* enantiomers. Finally, the subsequent *ortho*-borylation and methylation of **2b** yielded azabora[8]helicene **1b** with 64% overall yield. The last two steps are convenient for increasing the helicene's size from a hexa- to an octa-helicene. Both **2b** and **1b** were fully characterized (see SI). The ^1H NMR spectrum of the ligand **2b** shows for example the proton H^3 resonating at 6.79 ppm as a doublet of doublets due to coupling with the F atom ($^3J_{HF}$ = 9.3 Hz) and with H^2 (*J* = 8.3 Hz). For **1b**, the ^1H NMR demonstrates two upfield shifted signals for the diastereotopic methyl groups at −0.40 and −0.43 ppm and a doublet at 7.21 ppm corresponding to the proton H^3 ($^3J_{HF}$ = 8.9 Hz). The ^{11}B NMR displays one broad signal at −0.7 ppm and the ^{19}F NMR shows a doublet at −121.0 ppm, with the same $^3J_{HF}$ coupling constant of 9.3 Hz (coupling with H^3). Note that the NMR signals for the [8]helicene derivative appear at higher field than for the [6]helicene one, presumably due to the anisotropy cone effect of the longer helicene core.

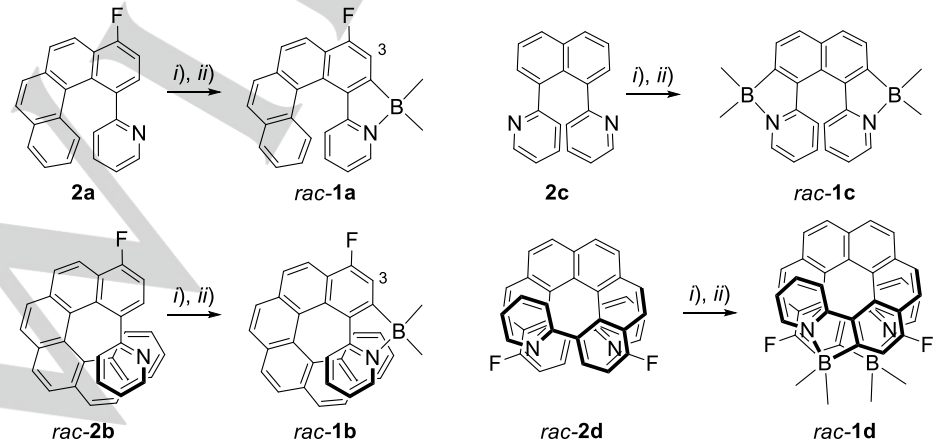

Scheme 2. Synthetic routes to azabora[*n*]helicenes **1a**-**d**. *i*) BBr_3, $N^iPr(Et)_2$, CH_2Cl_2, 25°C, 24 hrs; *ii*) $AlMe_3$, CH_2Cl_2, 30 min.

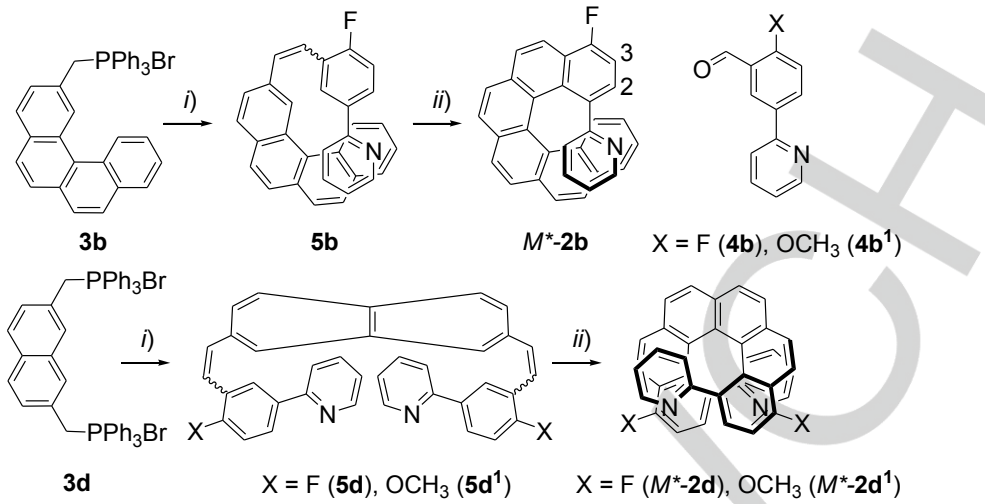

Scheme 3. Synthesis of racemic ligands **2b**, **2d** and **2d**[1]. *i*) **4b** or **4b**[1], *n*-BuLi, THF, Ar, r.t., 2 hrs; *ii*) *hv*, cat. I_2, air, toluene, 16 hrs.[$]

Racemic bis-azabora[6]helicene **1c** was prepared in two steps from the already known ligand **2c**[8e] in 55% overall yield according to the procedure presented in Scheme 2. This double cycloborylation enables a [6]helicene incorporating two boron atoms to be obtained in a straightforward manner from a 1,8-bi-pyridyl-naphthalene scaffold. The ^{1}H NMR of **1c** is in agreement with a C_2-symmetric molecule and shows two upfield shifted signals for the diastereotopic methyl groups at 0.31 and 0.10 ppm. The ^{11}B NMR displays one broad signal at 0.5 ppm. Single crystals of (±)-**1c** were grown by slow diffusion of pentane vapors into a CH_2Cl_2 solution and its structure was further ascertained by X-ray crystallography. Compound (±)-**1c** crystallized in the centro-symmetric *I*2/*a* space group (*i.e.* with the presence of both *P* and *M* enantiomers, Figure 2). The molecular structure shows a C_2 symmetry with a helicity (dihedral angle between terminal rings) of 53.1°, a typical value for a [6]helicene.[3] The C11−B1 and the B1−N1 bond-lengths are 1.598 and 1.617 Å respectively, which is in the range of similar 4-coordinate boron derivatives.[7] Heterochiral supramolecular columns formed of alternating *M* and *P* helices due to intermolecular π–π stacking are observed (Figure 2b). Furthermore, similarly to what was observed when comparing mono- and bis-platina[6]helicenes,[8e] the [6]helicenic **1c** has a more open helical structure than the mono-azabora[6]helicene **1a** because of the presence of two azaboracycles. This structural feature, along with a possible lability of the B-N bond, lead to a low configurational stability of **1c** in solution at room temperature and to its easy racemization (*vide infra*).

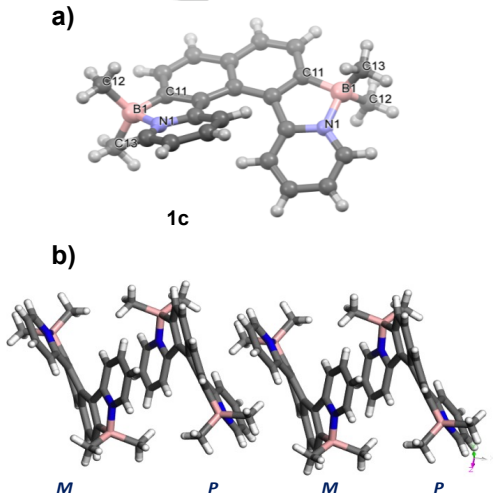

Figure 2. a) X-ray structure of (±)-**1c** (only the *P* enantiomer is shown) along with b) its heterochiral supramolecular arrangement along the *x* axis.

The preparation of [*n*]helicenes with *n* higher than 8 is still very challenging.[11] Taking advantage of the 4-cycles increase upon the double cycloborylation, we examined the preparation of bis-azabora[10]helicene **1d** from the [6]helicene ligand **2d** substituted with two 2-pyridyl groups in the inner 1,16 positions. **2d** was prepared as demonstrated in Scheme 3. A double Wittig reaction performed on aldehyde **4b** and naphtha-2,7-diyl-bis-triphenylphosphonium-*bis*-bromide salt **3d**[10b,c] yielded the bis-stilbenic compound **5d**. Then, a double photocyclization under irradiation by a mercury lamp and in the presence of a catalytic amount of iodine in a highly diluted toluene solution produced racemic **2d** in 11% yield. The low yield of the last photocyclization step can be explained by high steric hindrance since both of the inner positions, *i.e.* 1 and 16, are substituted by a 2-pyridyl group. As **2b**, carbo[6]helicene derivative **2d** is configurationally stable and exists as a racemic mixture of both *P* and *M* enantiomers. The ^{1}H NMR spectrum of **2d** is typical of a C_2-symmetric [6]helicene system (see SI). Single crystals of (±)-**2d** were grown by slow diffusion of pentane vapors into a

CH_2Cl_2 solution, and the structure was resolved by X-ray diffraction. The compound crystallizes in the centrosymmetric $P2_1/a$ space group (Figure 3a,b) with the presence of both *P* and *M* enantiomers in the unit cell. The helicity of the **2d** [6]helicene moiety is 31.9°, which is small and may be explained by π-π stacking interactions between each terminal pyridyl ring with the helicene backbone (centroid-centroid distances of 3.38-3.59 Å between the pyridyls and the second fused phenyls, see Figure 3a). Note also that the two nitrogen atoms are placed in the outer side and that the pyridyl rings and the helicene's terminal rings are not coplanar (dihedral angles of 32.3-44.9°). Furthermore, heterochiral supramolecular columns formed of alternating *M* and *P* helices are observed (Figure 3b). The racemic bis-azabora[10]helicene (±)-**1d** was finally prepared from (±)-**2d** by a double cycloborylation (66% overall yield, Scheme 2). The ^{1}H NMR of **1d** is in agreement with a C_2-symmetric structure and shows two shielded signals at 0.06 and −0.52 for the BMe_2 group. The ^{11}B NMR demonstrates one shielded signal at -0.6 ppm, and the ^{19}F NMR displays a doublet due to the coupling with the H^3 proton (-119.5 ppm, $^3J_{HF}$ = 8.8 Hz). Complex (±)-**1d** crystallizes in the centrosymmetric $P\bar{1}$ space group (Figure 4). The helicity of this molecule is very small, *i.e.* 2.6° which may be due to the strong π-π stacking between the 4 terminal rings of each side (smallest centroid-centroid distance: 3.67 Å). The distance between two boron atoms is 6.19 Å. Note that the deca-helicene **1d** forms a helix bigger than 1½ turn. The supramolecular arrangement of **1d** is similar to that of **2d** and **1c**, with heterochiral supramolecular columns formed of alternating *M* and *P* helices along the *y* axis. Furthermore, close CH_3-π contacts are present between the BMe_2 groups and one phenyl of the neighbouring helicene (Figure 4b).

Similarly to (±)-**2d**, ligand (±)-**2d^1** bearing two methoxy groups was synthesized in two steps from **3d** and using **4d^1** as the aldehyde precursor (Scheme 3). As in the case of **2d**, the yield of the photocyclization step was low (19%) due to high steric hindrance. Ligand **2d^1** displays the same characteristics as **2d** (see SI). For example, the **2d^1** crystallizes in the centrosymmetric $P\bar{1}$ space group with a helicity value of 36.9°, which is again relatively small due to the π-π stacking of each terminal pyridyl ring with the helicene backbone (centroid-centroid distances of 3.52 Å between the pyridyls and the second fused phenyls, see Figure 3c). Furthermore, the two nitrogen atoms are also placed in the outer side. In the case of **2d^1**, homochiral supramolecular columns formed from either *M* or *P* enantiomers are observed (Figure 3d).

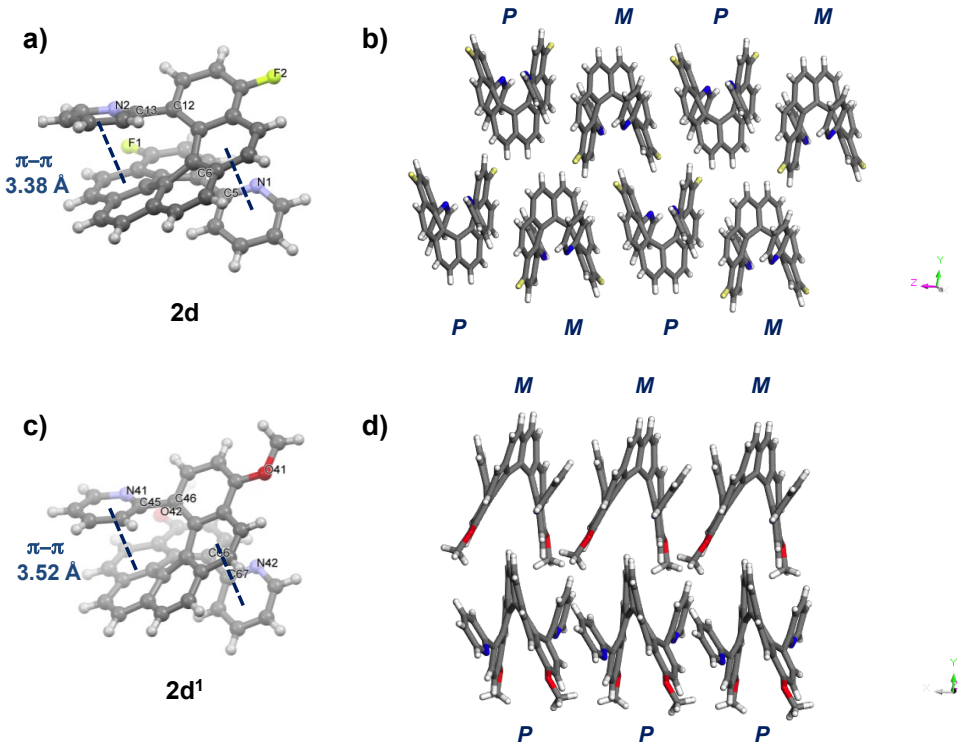

Figure 3. X-ray structures of a) (±)-**2d** and c) (±)-**2d^1** (only the *P* enantiomers are shown) along with their corresponding b) heterochiral and d) homochiral supramolecular arrangement along the *z* and *x* axis, respectively.

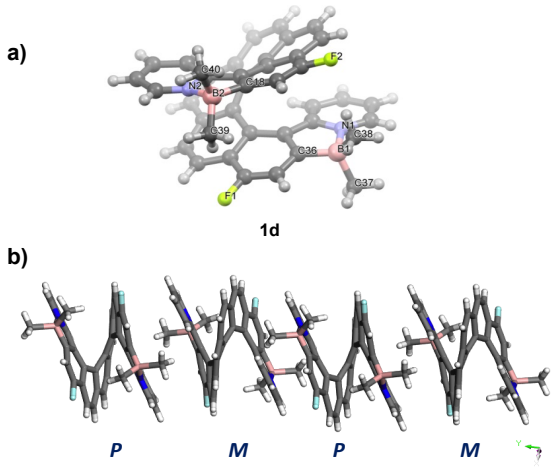

Figure 4. a) X-ray structure of (±)-**1d** (only the *M* enantiomer is shown) along with b) its corresponding heterochiral supramolecular arrangement along the *y* axis.

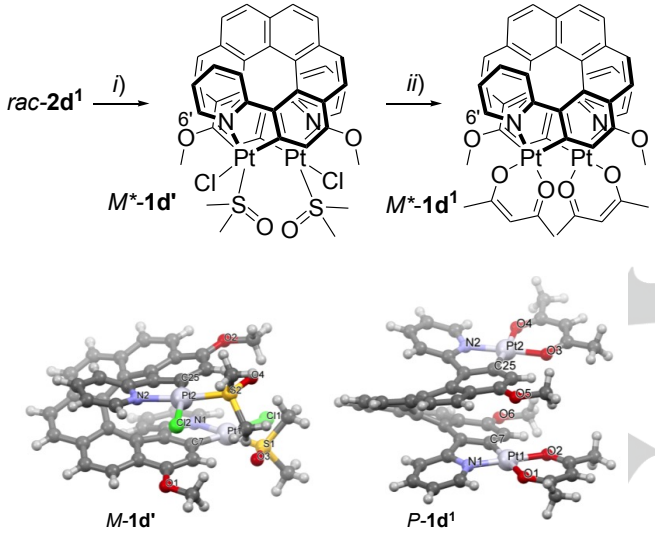

Scheme 4. Synthesis and X-ray structures of bis-platina[10]helicenes **1d'** and **1d**[1].[$] *i*) $Pt(dmso)_2Cl_2$, Na_2CO_3, toluene, reflux, 84%; *ii*) acacNa, toluene, reflux, 57%.

Finally, the bisplatina[10]helicene **1d**[1] was synthesized in its racemic form by using a double cycloplatination (Scheme 4). First, intermediate (±)-**1d'** bearing two chloro and two dimethyl sulfoxide (dmso) ancillary ligands was obtained with 84% yield by reacting the ligand **2d**[1] with 3 eq. of $Pt(dmso)_2Cl_2$ in the presence of 6 eq. of Na_2CO_3 in refluxing toluene at 110 °C. The final racemic complex **1d**[1] bearing two acetylacetonato ligands was then obtained by reacting (±)-**1d'** with sodium acetylacetonate in refluxing toluene at 110 °C in ca. 57% yield. Both complexes **1d** and **1d**[1] were fully characterized (see SI). Single crystals of (±)-**1d'** were obtained by slow diffusion of pentane vapors into a CH_2Cl_2 solution, and the structure was solved by X-ray diffraction. This intermediate system crystallizes in the centrosymmetric *C*2/*c* space group (both *P* and *M* enantiomers in the unit cell), and the structure shows ten *ortho*-fused rings with intramolecular π-π stacking between the last 4 terminal rings on each side (smallest centroid-centroid distance: 3.37 Å). For this reason, the helicity of **1d'** is only 18.7°. Furthermore, the distance between the two platinum atoms is small (4.83 Å). The ^{1}H NMR spectrum of **1d**[1] is characteristic of a C_2-symmetric structure. For instance, **1d**[1] displays the typical satellite peaks due to the coupling with ^{195}Pt ($^3J_{Pt\text{-}H}$ = 32 Hz) for the 6'-protons in the two pyridyl groups. Single crystals were obtained by slow diffusion of pentane vapors into CH_2Cl_2 solution of (±)-**1d**[1], and the structure was resolved by X-ray diffraction. The complex crystallized in the non-centrosymmetric $P2_1$ space group which means that there is a spontaneous resolution to pure *M*- and *P*-**1d**[1]. The helicity of this [10]helicene is small (22.0°). Besides, π-π stacking can also be observed in this molecule between the 4 terminal rings in each side (smallest centroid-centroid distance: 3.46 Å). The distance between the two Pt atoms is 5.94 Å, almost 1 Å bigger than the value in **1d'**, but similar to the B-B bond distance in **1d** (6.19 Å). It is important to note that the deca-helicenes **1d'** and **1d**[1] form a helix with more than 1½ turns and that, within the helix, the two platinacycles are facing each other and are therefore in an almost non-chiral local environment. This has a strong impact on the chiroptical properties (*vide infra*).

Photophysical properties

UV-vis spectroscopy

The UV-vis spectra of the azabora[*n*]helicenes **1a**-**d** were measured in CH_2Cl_2 solution at concentrations ca. 10^{-4} mol·L^{-1} and analyzed in detail with reference to corresponding platina[*n*]helicenes data (Table 1, Figures 5a,b and 6a,b, SI).[£] The **1a** system displays a set of intense structured bands (ε > 26000) centered at 237 and 263 nm, and structured bands of moderate intensity (ε ~ 5000-10000) between 359-398 nm (Figure 5a, Table 1). The increase in the helicene's size from a hexa- to an octa-helicene leads to an increase in the intensity of the absorption bands of **1b** and a bathochromic shift (ca. 30 nm) of its lower-energy band as compared to **1a**. Indeed, mono-azabora[8]helicene **1b** demonstrates a sharp absorption band at 232 nm (ε > 53900) accompanied by a shoulder at 265 nm (ε ~ 47000), and a set of strong structured bands between 324-374 nm (ε ~ 10000-25000), and bands of weaker intensity at 404 and 429 nm (1500-2500). Overall, the bis-azabora[6]helicene **1c** shows absorption bands similar to those of **1a** but the intensities are weaker between 230-330 nm and stronger between 330-430 nm. Again, the increase in the helicene's size from a hexa- to a deca-helicene results in much stronger absorption for **1d** than for **1c**, with intense bands at 269, 337 and 377 nm (ε ~ 60000, 31000 and 12400, respectively), and weaker bands at 415 and 440 nm (ε ~ 3000-4000) that are ca. 50 nm red-shifted compared to **1c**. Note that overall, the UV-vis spectrum of bis-azabora[10]helicene **1d** resembles that of the mono-azabora[8]helicene **1b**, with increased intensity and red-shift consistent with an elongation of the π-conjugated system from an [8]helicene to a [10]helicene. Compared to **1a**-**d**, the corresponding cycloplatinated derivatives **1a**[1]-**d**[1] show very similar (although generally of stronger intensity) UV-vis bands at higher-energy spectral regions, but with additional moderate or weak absorption bands in the low-energy region, *i.e.* above 430 nm (Figure 6a,b).[8a,b,e] In particular, in newly synthesized bis-platina[10]helicene **1d**[1] the lowest-energy band occurs at 480 nm with a tail down to 520 nm.

UV-vis spectra of **1a**-**d** and **1d**[1] were calculated by time-dependent DFT (LC-PBE0* functional with a continuum solvent model for CH_2Cl_2 at DFT BP-D3 geometries)[12] and agree very

well with experiment (Figure 5b, see SI for computational details and a full set of computed data). A detailed excitation analysis in terms of molecular orbital (MO) pair contributions of azabora[*n*]helicenes **1a-d** shows that the first electronic excitations are responsible for lowest-energy bands and that they are of π-π* type and involve the HOMO / LUMO pair (*P*-**1a**: 78%, *P*-**1b**: 56%, *P*-**1c**: 97%, *P*-**1d**: 42%) and the HOMO-1 / LUMO+1 pair in the case of more π-extended azabora[8]helicene **1b** (23%) and azabora[10]helicene **1d** (32%). As shown in Figure 7, for all azaborahelicenes studied here the HOMO and LUMO are π-conjugated throughout the molecule, including the boracycle and the pyridine moieties. As may be expected, orbitals of the electron-deficient boron atoms do not directly contribute to the π-electron system (*vide infra*). The additional contributions from the HOMO-1 / LUMO+1 pairs in the excitations of **1b** and **1d** indicate a partial charge-transfer (CT) character. This correlates with an observed red-shift of the lowest-energy excitations of **1b** and **1d** as compared to **1a** and **1c**. For the bis-azabora[6]helicene **1c** there are other excitations that contribute to the longest-wavelength absorption band, *e.g.* no. 2 and 3. These excitations exhibit some contributions from HOMO-1. Interestingly, this orbital clearly shows a conjugation between the B-CH_3 σ-bonds and the π-system of the naphthalene scaffold (see Figure 8). Other **1c** MOs with similar features but involving the whole C^N π-skeleton were also identified, but they have much lower orbital energies and are not involved to any significant degree in the low-energy electronic excitations. Similar, albeit less pronounced, mixing of B-CH_3 σ-bonds and orbitals of the π-system of the C^N helical scaffold was found for all remaining azaborahelicenes considered here (Figure 8, SI). The pronounced mixing in the HOMO-1 of **1c** leads to low-energy electronic excitations with some charge transfer character from B-CH_3 σ-bonds to the π-conjugated electron system, which may account for the increase in the low-energy absorption intensity of **1c** compared to **1a**.

The question presents itself whether there are covalent interactions involving B-CH_3 fragment σ-orbitals and C^N fragment π-orbitals that goes along with the mixing of these orbitals in the canonical (*i.e.* self-consistent field (SCF)) MOs of the azaborahelicenes, or if the mixing is driven by other effects such as a (near-)degeneracy of the fragment orbitals. Accordingly, to gain deeper insight into the effect of the presence of the boron atom(s) on the helicene π-system, a quantum-chemical analysis of the electronic structures of **1a-d** was performed with the natural bond orbital (NBO) method. The NBO analysis revealed a stabilizing electron delocalization between σ(B-C(CH_3)) and antibonding π*-(C^N) fragment orbitals. Such interactions are commonly associated with σ-π hyperconjugation (SI).

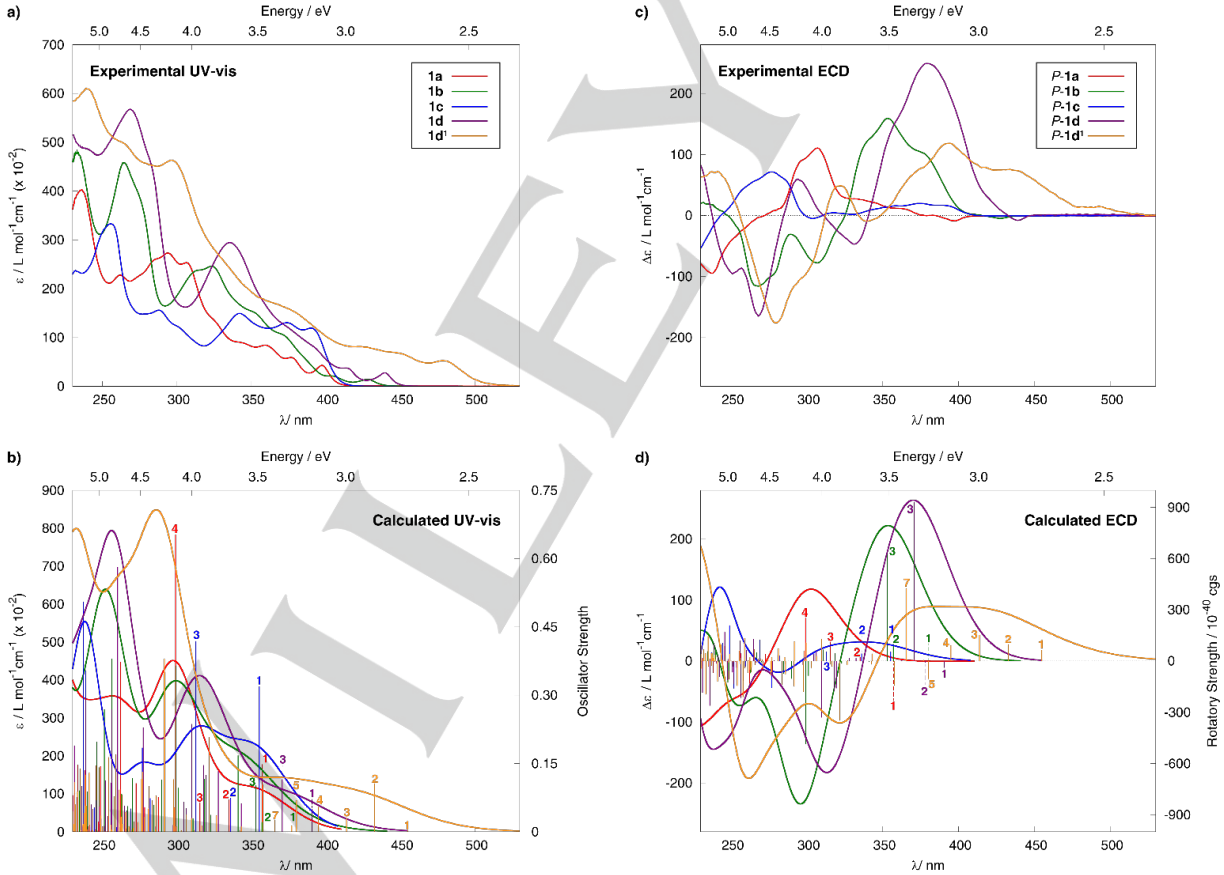

Figure 5. Experimental UV-vis (panel a) and ECD (panel c) spectra of azaborahelicenes *P*-**1a-d** and of bis-platina[10]helicene complex *P*-**1d'** (CH_2Cl_2, C $1 \cdot 10^{-4}$ M) and their corresponding simulated spectra (panels b and d, respectively). TDDFT LC-PBE0* calculations with continuum solvent model for dichloromethane at BP-D3 optimized geometries. No spectral shift has been applied. Calculated excitation energies and rotatory strengths indicated as 'stick' spectra. Numbered excitations correspond to those analyzed in detail (see SI).

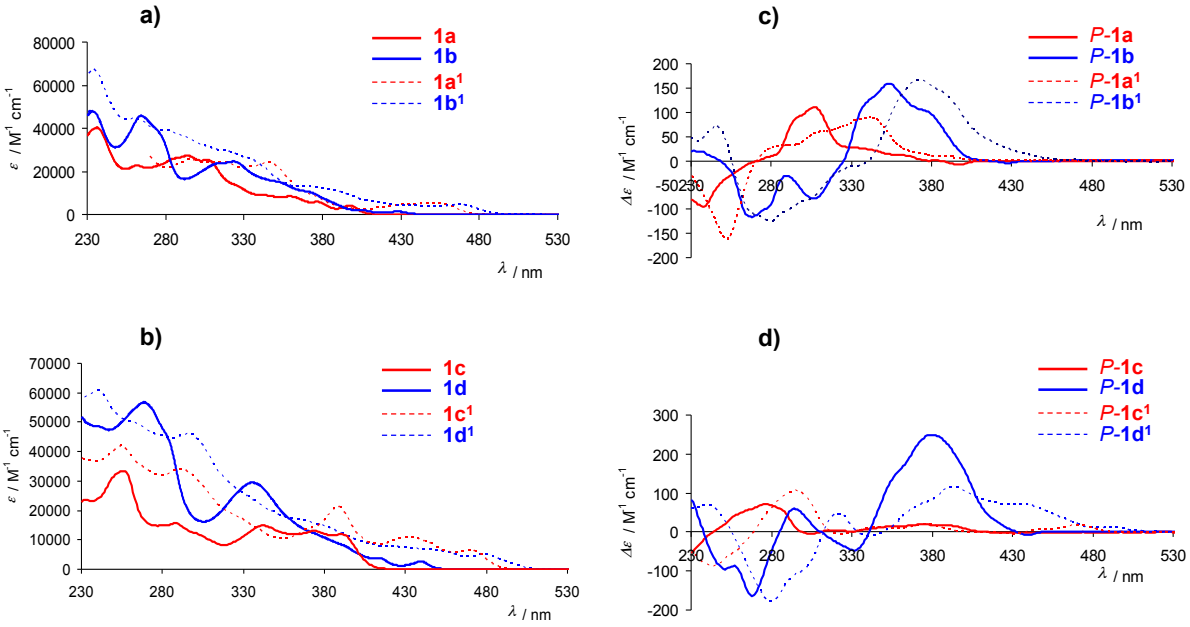

Figure 6. Comparison of the experimental UV-vis (panels a and b) and ECD spectra (panels c and d) of *P* enantiomers of azaborahelicenes **1a-d** and the corresponding platinahelicenes **1a**[1]-**1d**[1].[8a,b,e]

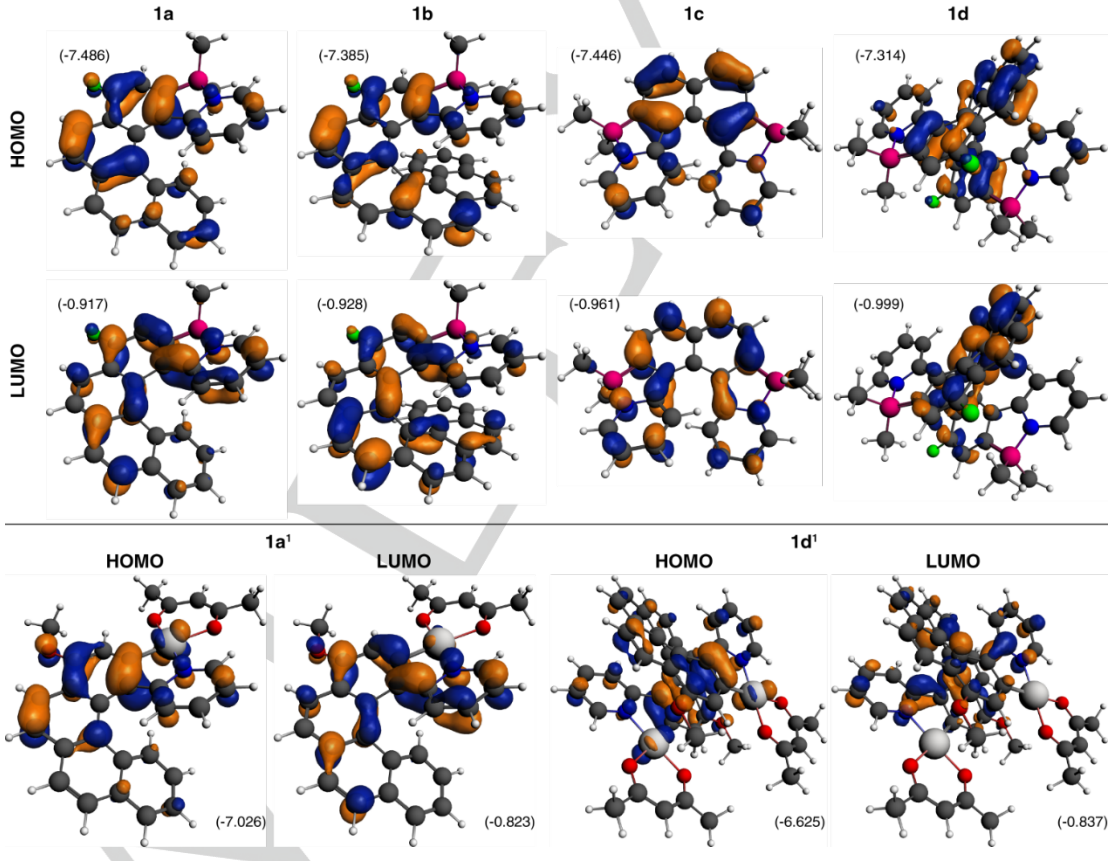

Figure 7. Isosurfaces (0.04 au) of HOMOs and LUMOs of the azaborahelicene systems **1a-d** (top) and platinahelicene complexes **1a**[1] and **1d**[1] (bottom). Values listed in parentheses are the corresponding orbital energies, in eV. LC-PBE0*//BP-D3 calculations with continuum solvent model for dichloromethane.

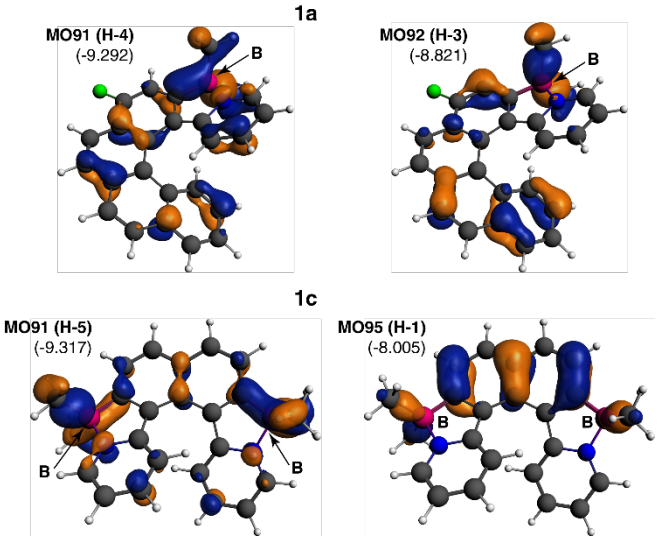

Figure 8. Isosurfaces (0.04 au) of selected MOs of the azaborahelicene systems **1a** (top) and **1c** (bottom) demonstrating σ-π mixing (for full set of MOs see SI). Values listed in the parentheses are the corresponding orbital energies, in eV. LC-PBE0*//BP-D3 calculations with continuum solvent model for dichloromethane. 'H' = HOMO.

As already shown for platina[*n*]helicenes **1a**^{1}-**c**^{1}, Pt centers may efficiently interact with extended azahelicene π-orbitals (see Figure 7 for frontier orbitals of **1a**^{1}) which is reflected in the presence of additional low-energy absorption bands observed for such systems.[8a,b,e] The quantum-chemical analysis of **1d**^{1} revealed similar electronic features. The excitation at lower energy with sizable dipolar oscillator strength (no. 2) has a large contribution from the HOMO-1 / LUMO (75%) pair and a secondary one from HOMO / LUMO+1 (13%) and may therefore be assigned as a π-π* transition with some participation of the platinum 5*d* orbitals. This finding is in full agreement with the previous assignments for **1a**^{1}-**c**^{1}.[8a,b,e]

To summarize: (*i*) All four novel heteroatomic helicenes reveal generally similar UV-vis spectra whose intensity and energy changes are typical for an enlargement of the [*n*]helicene π-electron system along the series. (*ii*) Unlike the platina[*n*]helicenes **1a**^{1}-**d**^{1} cases, where metal atoms do not only construct the helicoidal framework by double orthometallation but also markedly impact the electronic properties of the π-conjugated system, the effect of the cycloboration seems to be primarily to increase the size of the helicene skeleton by systematically adding two *ortho*-fused cycles and to involve these two cycles in the electronic π–π* type transitions. Overall, compounds **1a**-**d** appear thus to behave as classical organic [*n*]helicene derivatives, but with additional σ-π hyperconjugation associated with the boron centers.

Luminescence properties

The luminescence properties of azabora[*n*]helicenes **1a**-**d** and bis-platina[10]helicene **1d**^{1} were measured in CH_2Cl_2 at 298 K (room temperature, r.t.) and in EPA at 77 K (EPA = diethyl ether/isopentane/ethanol, 2/2/1 *v*/*v*). The results are summarized in Table 1 and the r.t. emission spectra are displayed in Figure 9. Additional spectra including those at 77 K are provided in the SI. All four azaborahelicenes reveal a moderate to intense blue fluorescence around 430-460 nm at 298 K, with relaxation times of a few nanoseconds, and quantum yields between 7-49%. The [6]helicene derivatives with one (**1a**) and two azaboracycles (**1c**) demonstrate higher quantum yield, 21% and 49%, respectively; the latter being quite high for [6]helicenes[3f,g] and consistent with the results for other azaborole derivatives.[9b-d] The increase in the helicene's size from hexa- to octa- and deca-helicenes leads to smaller quantum yields (~ 7%). At low temperature, all four borahelicenes show green phosphorescence with relaxation times around 1 s, a behavior previously observed in organic helicenes.[3f,g] The Pt_2-[10]helicene **1d**^{1} displays a red phosphorescence (see Table 1) around 640 nm at 298 K with a relaxation time of 27 μs and a moderate quantum yield (~ 7%). This corresponds to the typical emission properties of platinahelicenes, such as the previously studied **1a**^{1}-**c**^{1}.[8e]

The calculated (LC-PBE0*, CH_2Cl_2 solvent model) fluorescence and phosphorescence energies for **1a**-**d** correspond well with measured low-temperature data, supporting the experimental assignment (see SI). Similarly, in the case of bis-platina[10]helicene **1d**^{1} the calculated energy of $S_1 \rightarrow S_0$ fluorescence transition differs significantly from that of the experimental luminescence, while the phosphorescence energy $T_1 \rightarrow S_0$ agrees very well with experiment. For all the systems the calculated optimized excited states S_1 and T_1 and ground states S_0 are structurally very similar (SI).

Chiroptical properties (electronic circular dichroism, optical rotation)

The electronic circular dichroism (ECD) spectra and optical rotation (OR) parameters of azabora[*n*]helicene derivatives **1a**-**d** and bis-platina[10]helicene complex **1d**^{1} were examined next (Figures 5c,d and 6c,d, Table 2, SI).[£] The *M* and *P* enantiomers of each helicene derivative were obtained with *ee*'s between 96.0-99.5% through HPLC separations over a chiral stationary phase, and, as expected, they displayed mirror-image ECD spectra (see SI). Note that bis-azabora[6]helicene **1c** easily racemizes in solution and a 25% loss of the optical rotation was observed for this compound, upon leaving the enantiopure *M*-**1c** or *P*-**1c** in CH_2Cl_2 solution for one week at room temperature. An inversion barrier $\Delta G^{\neq}$ of 114.9 kJ mol^{-1} (78°C, ethanol) was experimentally estimated by racemization kinetic studies (see SI). Consequently, a freshly prepared solution was used systematically for the optical measurements.

The azabora[6]helicene *P*-**1a** shows typical ECD[£] of [6]helicene derivatives, *i.e.* a strong negative band at 237 nm ($\Delta\varepsilon$ = −95) along with two strong positive bands at 296 (+89) and 307 nm (+110), accompanied with an additional weak negative one at 397 nm (−8.7), see Figure 5c. The π-elongated azabora[8]helicene *P*-**1b** displays an ECD spectrum that is more intense and significantly red-shifted (ca. 50 nm) compared to **1a**, with for example two strong negative ECD-active bands at 267 ($\Delta\varepsilon$ = −116) and 307 nm (−77), three strong positive bands at 340 (+122), 353 (+159), and 379 nm (+100), and, similarly to *P*-**1a**, an additional very weak negative band at 427 nm (−4.8). In spite of a general similarity between the **1a** and **1c** UV-vis spectra (*vide supra*), the bis-azabora[6]helicene *P*-**1c** exhibits an ECD spectrum that significantly differs from those for typical helicene derivatives. It displays a strong positive band at 277 ($\Delta\varepsilon$ = +71), a very weak negative intensity at 303 (−4.8) that is followed by three positive bands of medium intensity at 358 (+15), 374 (+20), and 392 nm (+16). Overall the ECD of **1c** is

relatively weak for a [6]helicene derivative. On the contrary, bis-azabora[10]helicene *P*-**1d** shows very strong and red-shifted (> 30 nm) ECD compared to *P*-**1a**-**c**, fully consistent with an elongation of the π-conjugated system. The compound reveals two strong negative bands at the 251 ($\Delta\varepsilon$ = −95) and 268 nm (−165), positive and negative ones of medium intensity at respectively 294 (+59) and 331 nm (−47), and strong positive band at 379 nm (+249). As for mono-azaborahelicenes *P*-**1a** and *P*-**1b**, an additional weak negative intensity occurs at lowest-energy part of the *P*-**1d** spectrum (439 nm, $\Delta\varepsilon$ = −7.9).

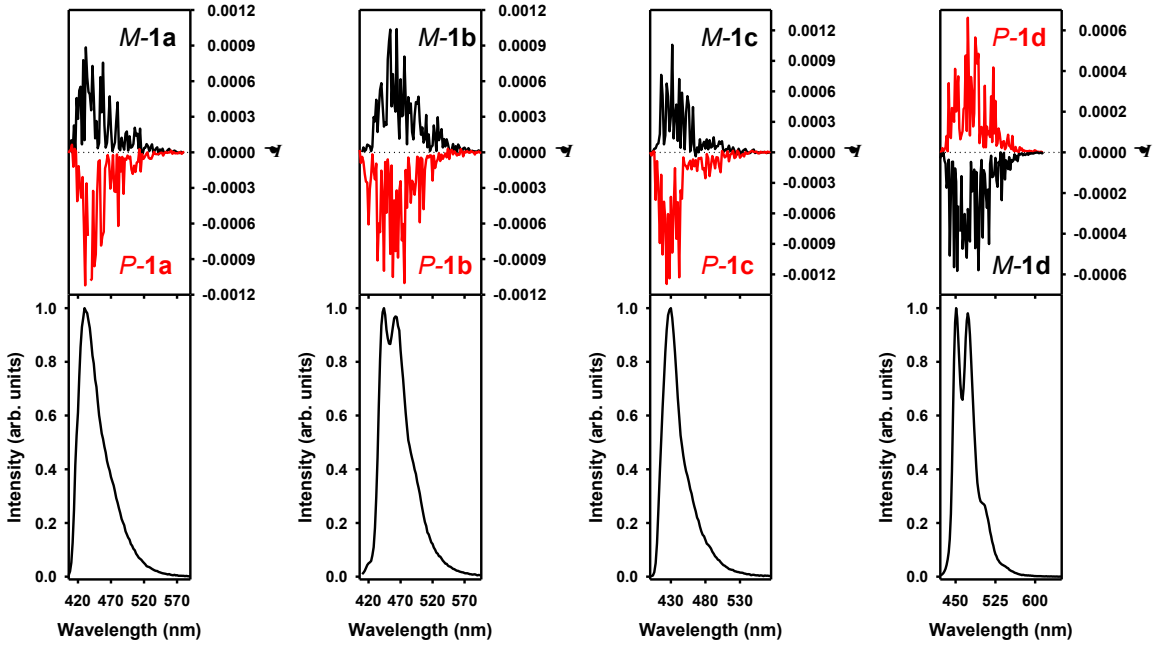

Figure 9. The CPL spectra (upper) and the luminescence spectra (lower) for both enantiomers of azaborahelicene **1a** (λ_{ex} = 395 nm), **1b** (λ_{ex} = 405 to 409 nm), **1c** (λ_{ex} = 405 nm), and **1d** (λ_{ex} = 420 nm) measured in CH_2Cl_2 at r.t. (see also SI).

Table 1. UV-vis and emission data for azaborahelicenes **1a**-**d** and the related Pt_2 complex **1d**[1] (in CH_2Cl_2 at 298 K or EPA at 77 K).

Compound	Absorption λ_{max} / nm (ε / $M^{-1}cm^{-1}$)	Emission r.t. λ_{max} / nm	Φ [a]	τ / ns	Emission 77 K	
					λ_{max} / nm	τ / ns
1a	237 (46000), 263 (26400), 295 (33100), 307 (30400), 344 (10300), 359 (9740), 377 (6910), 398 (5250)	404, 425, 450sh	0.21	4.1	F: 396, 417, 443, 471	7.2
					P: 543, 581, 626	1.1×10^9
1b	232 (53900), 265 (46700), 324 (25500), 352sh (15800), 374sh (10500), 404 (2190), 429 (1440)	435, 458	0.069	5.3	F: 427, 454, 484, 516	7.3
					P: 546, 593, 643	1.2×10^9
1c	256 (49300), 288 (18200), 342 (18100), 375 (15600), 391 (14300)	427	0.49	3.2	F: 397, 415, 443, 474sh	3.9
					P: 556, 604, 654	0.62×10^9
1d	269 (60200), 337 (31200), 377sh (12400), 415 (4020), 440 (3000)	443, 471, 502, 541	0.074	5.5	F: 437, 464, 496, 532	7.3
					P: 554, 599, 657	1.1×10^9
1d[1]	242 (72400), 297 (57000), 368sh (20800), 426 (9250), 446 (8380), 479 (6850)	639, 663	0.066	27×10^3	P: 615, 665, 738sh	61×10^3

[a] Quantum yields of **1a**-**d** / **1d**[1] were measured using quinine sulfate or $[Ru(bpy)_3]^{2+}$ as standards: see S.I. 'F' – fluorescence. 'P' – phosphorescence.

The corresponding TDDFT simulated ECD envelopes for *P*-**1a**-**d** (LC-PBE0*//BP-D3, CH_2Cl_2 solvent model) agree in general, very well with the experiments. As shown in Figure 5d, important experimentally observed trends are correctly reproduced by the calculations. Namely, there is an increasing red-shift of the ECD spectra with the increase in the helicene's size from the hexa- (**1a**) to the octa- (**1b**) to the deca-helicene (**1d**), and the calculated **1c** spectrum significantly differs from the others. No low-energy bands of weak negative intensity were observed in the broadened calculated vertical ECD spectra of *P*-**1a**,**b**,**d**. The excitations data shows that the lowest-energy excitation (no. 1, SI) in each of these systems has a negative rotatory strength. However, this weak negative rotatory strength is over-powered by excitations of strong positive intensity at higher energy, and the broadened spectra do not afford a low-energy ECD band. As already mentioned, the lowest-energy excitations are predominantly involving the HOMO / LUMO pair, with additional HOMO-1 / LUMO+1 contributions in the case of **1b** and **1d** (*vide supra*, Figure 7 and SI). The intense positive ECD band of *P*-**1a** is dominated by excitations no. 3 and 4, calculated at 315 and 299 nm, respectively. Excitation no. 3 mainly involves the HOMO / LUMO+1 pair (70%) and is therefore assigned to a CT π-π* transition as it involves orbitals centered in different parts of the π-system. Excitation no. 4 has two contributions, from HOMO / LUMO+2 (53%) and from HOMO-1 / LUMO (33%), and can be assigned as π-π* with some CT character. In the case of *P*-**1b**, low-energy positive ECD band originates from two nearly degenerate excitations, no. 2 (calculated at 357 nm) and no. 3 (353 nm). These excitations involves predominantly the π-π* HOMO / LUMO+1 pair (no. 2 / 3: 71% / 12%) along with the CT- π-π* pairs HOMO / LUMO (no. 2 / 3: 17% / 59%) and HOMO-2 / LUMO (no. 3: 18%). Accordingly, the *P*-**1b** excitation with the strongest rotatory strength (no. 3) reveals a higher degree of CT character than in the case of **1a**, which may be responsible for a corresponding red-shift of the ECD band. A similar conclusion can also be drawn for *P*-**1d**, for which the first ECD band is dominated by excitation no. 3 with a very large-magnitude rotatory strength calculated at 371 nm involving π-π* orbital pairs with some CT character (HOMO-1 / LUMO+1 (52%) and HOMO / LUMO (32%)).

The substantial difference between the ECD of *P*-**1c** and the *P*-**1a**,**b**,**d** spectra can easily be related to the underlying excitations. The first broad positive ECD band of *P*-**1c,** of moderate intensity, is caused by three excitations calculated at 355 (no. 1), 336 (no. 2), and 313 nm (no. 3) with positive rotatory strength values that are lower than in the case of **1a**,**b**,**d** (see SI). Their general assignment of the excitations is similar to those of **1a**,**b**,**d**: Excitation no. 1 has almost pure π-π* HOMO / LUMO character, the excitations no. 2 and 3 can be assigned as π-π* with some CT character (HOMO / LUMO+1 (no. 2 / 3: 75% / 17%) and HOMO / LUMO (no. 2 / 3: 18% / 57%)). However, unlike for the other azaborahelicenes, the CT contributions in the latter excitations involve B-CH_3 σ-bonds due to involvement of HOMO-1 (*vide supra*).

As shown in Figure 6c,d, the previously studied[8a,b,e] platina[*n*]helicene derivatives **1a**^{1}-**c**^{1} have ECD spectra of similar magnitude as in **1a**-**c**, but strongly red-shifted (20-50 nm), and with an additional characteristic low-energy tail of the first ECD band (which is positive for the *P*-isomers). Similar features are also observed for the novel bis-platina[10]helicene **1d**^{1} complex, although in this case a decrease in the intensity compared to **1d** can be noticed (Figures 5c, 6d). The assignment of first positive ECD bands in **1a**^{1} and **1b**^{1} is similar to those described above for **1a** and **1b**, although for the π-π* transitions with CT character localized in the C^N π-system of platinahelicene complexes there is a clear involvement of metal orbitals. In particular, π-π* transitions with some participation of the Pt 5*d* orbitals are responsible for low-energy tails of ECD spectra in **1a**^{1},**b**^{1}.[8a,b,e] Similarly to *P*-**1c**, its platina-based analogue *P*-**1c**^{1} reveals moderate positive ECD intensity around 350 nm that is also dominated by metal-enhanced π-π* transitions with partial CT character. Interestingly, the excitation involves an MO that demonstrates a noticeable contribution from non-bonding orbitals of both Pt centers which become a part of the naphthalene π-system,[8e] thereby resembling features of the **1c** HOMO-1 shown in Figure 8. It therefore appears that the structural arrangement is conducive to an electronic (hyper)conjugation. The assignment of the ECD spectrum of newly synthesized **1d**^{1} remains in line with those of **1a**^{1}-**c**^{1}, *i.e*. it is dominated by π-π* transitions with some CT character and involvement of Pt centers orbitals. The low-energy tail of the first **1d**^{1} ECD band is caused by the first electronic excitation (455 nm) which nearly purely involves the HOMO / LUMO pair (94%).

Table 2. Experimental and calculated molar rotations, $[\phi]_D$,[£] of enantiopure azabora[*n*]helicene systems *P*-**1a**-**d** and of bis-platina[10]helicene complex *P*-**1d**^{1}.[a]

Method	1a	1b	1c	1d	1d^1
BHLYP//BP	6557	19359	5377	30601	35752
BHLYP//BP-D3	6091	16916	5146	25970	27491
LC-PBE0*//BP	6357	20011	5265	33194	38106
LC-PBE0*//BP-D3	5782	17134	4987	28008	29308
Expt. (23°C)	5062	13953	5209	32134	35500

[a] TDDFT response calculation // DFT geometry optimization method. Continuum solvent model for dichloromethane (DCM, ε = 8.9). See SI for a full set of data.

The trends in the ECD-active bands observed for *P*-**1a**-**d** and *P*-**1d**^{1} are clearly reflected in the corresponding molar optical rotation (MR) data (Table 2). The MR generally doubles with increase in the helicene size from a hexa- (**1a**) to an octa- (**1b**) to a deca-helicene (**1d**), which is in line with the red-shift and increasing intensity of first positive ECD bands along the series. Similarly, the bis-azabora[6]helicene **1b** and bis-platina[10]helicene **1d**^{1} demonstrate optical rotations of slightly increased magnitude compared to their mono-azabora[6]helicene and bis-azabora[10]helicene analogues **1a** and **1d**. The calculated data listed in Table 2 (see also SI) show a strong dependence of the **1a**-**d** and **1d**^{1} MRs on the functional and the optimized geometries used in the OR calculations, which is in agreement with previous observations for other helicene derivatives.[13] With all computational model considered, the results remain however qualitatively the same and demonstrate (*i*) a strong increase in MR when extending the π-chromophore within the series **1a** < **1b** < **1d** < **1d**^{1} in line with

experiment, and (*ii*) a noticeable lower MR value of **1c** compared to **1a**.

To summarize: (*i*) Azabora[*n*]helicenes **1a**, **1b**, and **1d** reveal an overall similar shape of the ECD spectra which resembles that of classical organic helicene derivatives. Furthermore, the increase in the helicene size when going from a [6] (**1a**) to an [8] (**1b**) to a [10]helicene (**1d**) leads to more intense and more red-shifted spectra, reflecting a well-known tendency for helicenes that is attributed to the enlargement of the π-electron system. This confirms that the primary role of the boron atom(s) is to assemble additional helicoidal cycles that can be involved in the electronic π-π* type transitions. (*ii*) Bis-azabora[6]helicene **1c** displays a significantly different ECD spectrum from **1a**,**b**,**d**. The TDDFT results indicate that this is due to excitations with CT character involving B-CH_3 σ-bonds and the π-conjugated system, mainly *via* HOMO-1 which shows a conjugation of B-CH_3 σ-orbitals and π-orbitals of the C^N backbone. (*iii*) The strong red-shift of the ECD spectra along with appearance of additional low-energy tail of first positive ECD band for platina[*n*]helicenes **1a**^{1}-**1d**^{1} compared to their azaborahelicene analogues **1a**-**1d** can be rationalized by an extended π-conjugation involving metal orbitals from one or two Pt centers.

Circularly polarized luminescence (CPL)

Circularly polarized luminescence (CPL) activity, which combines emission and chirality, is another appealing chiroptical property of organic chiral chromophores such as helicenic derivatives,[14] including borylated ones.[14i,j] There is a growing interest in CPL,[15] and CPL emitters have recently been incorporated into OLEDs to obtain circularly polarized (CP) OLEDs.[8d,g] The CPL of enantiopure *P*- and *M*-azaborahelicene derivatives **1a**-**d** and bis-platina[10]helicene **1d**^{1} was examined (Figure 9, Table 1, SI). For the azabora[*n*]helicenes studied, the measured g_{lum} are of the order of 10^{-3} to 10^{-4} (see Table S5), which is classical for organic helicenes. However, these heterohelicenes show overall more efficient emission properties than most organic helicene derivatives[14] since their quantum yields are rather high, especially in the case of **1a** and **1c** (*vide supra*). On the other hand, the CPL activity of the azaborahelicenes **1a**-**c** is different from their corresponding platinahelicenes **1a**^{1}-**c**^{1} which displayed CPL red-phosphorescence with g_{lum} values up to $+10^{-2}$ for *P*-**1a**^{1} that recently proved very efficient for producing CP-OLEDs.[8g] The signs of the CPL signals are interesting to note since for **1a**, **1b** and **1c**, the CPL is positive for the *M*-enantiomers while it is negative for the *P*-enantiomers, which is the opposite situation for the bis-azabora[10]helicene **1d**. Note that negative CPL signals are often obtained in substituted organic *P*-helicenes.[16] Finally, the CPL was found to be zero in the *P*- and *M*-**1d**^{1} which may be due to the square-planar geometry of the Pt atom that is mainly placed in a non-chiral environment and / or degradation upon the xenon lamp illumination. CPL simulations based on vertical transition energies and transition moments were also performed, but with inconsistent results (see SI). It is likely that the vibronic emission spectra need to be simulated[17] in order to replicate the experimental dissymmetry factors, which is beyond the scope of the present work.

Conclusions

In this paper, we have reported the synthesis of the first helical azaboroles by a straightforward cycloborylation of phenyl-pyridyl-type helicene π-ligands. The role of the boron atoms has been emphasized in (*i*) increasing the size of the helicenic structure up to an azabora[10]helicene, (*ii*) increasing the fluorescence quantum yield efficiency with quantum yields up to 50%, (*iii*) obtaining strong ECD and MR responses, (*iv*) introducing σ–π conjugation and π–π* charge transfers, (*v*) displaying CPL activity. These enantiopure compounds therefore demonstrate a behavior that is complementary to their corresponding cycloplatinated helicenes and may find applications in chiral optoelectronic devices.

Experimental Section

Experimental Details are described in the Supplementary Information.

Acknowledgements

We thank the Ministère de l'Education Nationale, de la Recherche et de la Technologie, the Centre National de la Recherche Scientifique (CNRS), the ANR (12-BS07-0004-METALHEL-01), the CHIRAFUN CNRS network, and the IAL (CNRS) Rennes-Durham for financial support. M.S.-H. is grateful for financial support from the Ministry of Science and Higher Education in Poland ('Outstanding Young Scientist' scholarship and young researchers' T-subsidy). J.A. acknowledges the National Science Foundation (CHE 1560881 and 1265833) for financial support and the Center for Computational Research (CCR) at the University at Buffalo for computational resources. G.M. thanks the NIH, Minority Biomedical Research Support (grant 1 SC3 GM089589-07) and the Henry Dreyfus Teacher-Scholar Award for financial support, whereas A.R.T. and A.J.R. thank the SJSU RISE program (NIH grant 5R25GM71381) for a research fellowship.

Keywords: azaborahelicenes • circular dichroism • luminescence • CPL • quantum-chemical calculations

Notes and references

$ *M** indicates the racemic mixture of *M* and *P* enantiomers.

£ All ε and Δε values in this work are given in units of M^{-1} cm^{-1}, all specific rotations in degree [dm (g cm^{-3})]$^{-1}$, and all molar rotations in degree cm^2 $dmol^{-1}$.

[1] a) A. C. Grimsdale, K. Müllen, *Angew. Chem. Int. Ed.* **2005**, *44*, 5592-5629; b) A. C. Grimsdale, J. Wu, K. Müllen, *Chem. Commun.* **2005**, 2197-2204; c) L. Schmidt-Mende, A. Fechtenkçtter, K. Müllen, E. Moons, R. H. Friend, J. D. MacKenzie, *Science* **2001**, *293*, 1119-1122; d) J. Wu, W. Pisula, K. Müllen, *Chem. Rev.* **2007**, *107*, 718-747; e) H. Seyler, B. Purushothaman, D. J. Jones, A. B. Holmes, W. W. H. Wong, *Pure Appl. Chem.* **2012**, *84*, 1047-1067.

[2] a) K. Müllen, J. P. Rabe, *Acc. Chem. Res.* **2008***, 41*, 511-520; b) A. Narita, X.-Y. Wang, X. Feng, K. Müllen, *Chem. Soc. Rev*. **2015**, *44*, 6616-6643.

[3] Selected reviews: a) R. H. Martin, *Angew. Chem. Int. Ed.* **1974**, *13*, 649-660; b) T. J. Katz, *Angew. Chem. Int. Ed.* **2000**, *39*, 1921-1923; c) A. Urbano, *Angew. Chem. Int. Ed*. **2003**, *42*, 3986-3989; d) A. Rajca, M. Miyasaka, in *Functional Organic Materials* (Eds.: T. J. J. Müller, U. H. F. Bunz), Wiley-VCH, Weinheim, **2007**, pp. 543-577; e) F. Dumitrascu, D. G. Dumitrescu, I. Aron, *Arkivoc* **2010**, 1-32; f) Y. Shen, C. -F. Chen, *Chem. Rev.* **2012**, *112*, 1463-1535; g) M. Gingras, *Chem. Soc. Rev.* **2013**, *42*, 1051-1095; h) J. Bosson, J. Gouin, J. Lacour, *Chem. Soc. Rev.* **2014**, *43*, 2824-2840; i) N. Saleh, C. Shen, J. Crassous, *Chem. Sci.* **2014**, *5*, 3680-3694.

[4] a) H. Hirai, K. Nakajima, S. Nakatsuka, K. Shiren, J. Ni, S. Nomura, T. Ikuta, T. Hatakeyama, *Angew. Chem. Int. Ed.* **2015***, 54*, 13581-13585; b) K. Schickedanz, T. Trageser, M. Bolte, H.-W. Lerner, M. Wagner, *Chem. Commun.* **2015**, *51*, 15808-15810; c) T. Hatakeyama, S. Hashimoto, T. Oba, M. Nakamura, *J. Am. Chem. Soc.* **2012**, *134*, 19600-19603; d) Y. Si, G. Yang, *J. Mater. Chem. C* **2013**, *1*, 2354-2361.

[5] a) X. -Y. Wang, J. -Y. Wang, J. Pei, *Chem. Eur. J.* **2015**, *21*, 3528-3539 and references therein; b) P. G. Campbell, A. J. V. Marwitz, S. -Y. Liu, *Angew. Chem. Int. Ed.* **2012**, *51*, 6074-6092; c) Z. Liu, T. B. Marder, *Angew. Chem. Int. Ed.* **2008**, *47*, 242-244; d) S. Yamaguchi, A. Wakamiya, *Pure Appl. Chem.* **2006**, *78*, 1413-1424; e) F. Jäkle, *Chem. Rev.* **2010**, 110, 3985−4022; f) A. Lorbach, A. Hübner, M. Wagner, *Dalton Trans.* **2012**, *41*, 6048-6063; g) A. Escande, M. J. Ingleson, *Chem. Commun.* **2015**, *51*, 6257-6274.

[6] a) D. Li, H. Zhang, Y. Wang, *Chem. Soc. Rev.* **2013**, *42*, 8416-8433; b) Y.-L. Rao, H. Amarne, S. Wang, *Coord. Chem. Rev.* **2012**, *256*, 759−770 and references therein

[7] a) Y. -L Rao, S. Wang, *Inorg. Chem.* **2011**, *50*, 12263-12274 and references therein; b) Y. -L Rao, H. Amarne, S. B. Zhao, T. M. McCormick, S. Martic, Y. Sun, R. Y. Wang, S. Wang, *J. Am. Chem. Soc.* **2008**, *130*, 12898-12900; c) C. Baik, Z. M. Hudson, H. Amarne, S. Wang, *J. Am. Chem. Soc.* **2009**, *131*, 14549-14559; d) V. F. Pais, M. M. Alcaide, R. López-Rodríguez, D. Collado, F. Nájera, E. Pérez-Inestrosa, E. Álvarez, J. M. Lassaletta, R. Fernández, A. Ros, U. Pischel, *Chem. Eur. J.* **2015**, *21*, 15369-15376.

[8] a) L. Norel, M. Rudolph, N. Vanthuyne, J. A. G. Williams, C. Lescop, C. Roussel, J. Autschbach, J. Crassous, R. Réau, *Angew. Chemie Int. Ed.* **2010**, *49*, 99-102; b) E. Anger, M. Rudolph, L. Norel, S. Zrig, C. Shen, N. Vanthuyne, L. Toupet, J. A. G. Williams, C. Roussel, J. Autschbach, J. Crassous, R. Réau, *Chem. Eur. J.* **2011**, *17*, 14178-14198; c) E. Anger, M. Rudolph, C. Shen, N. Vanthuyne, L. Toupet, C. Roussel, J. Autschbach, J. Crassous, R. Réau, *J. Am. Chem. Soc.* **2011**, *133*, 3800-3803; d) C. Shen, E. Anger, M. Srebro, N. Vanthuyne, L. Toupet, C. Roussel, J. Autschbach, R. Reau, J. Crassous, *Chem. Eur. J.* **2013**, *19*, 16722-16728; e) C. Shen, E. Anger, M. Srebro, N. Vanthuyne, K. K. Deol, T. D. Jefferson Jr., G. Muller, J. A. G. Williams, L. Toupet, C. Roussel, J. Autschbach, R. Réau, J. Crassous, *Chem. Sci.* **2014**, *5*, 1915-1927; f) O. Crespo, B. Eguillor, M.A. Esteruelas, I. Fernandez, J. Garcia-Raboso, M. Gomez-Gallego, M. Martin-Ortiz, M. Olivan, M.A. Sierra, *Chem. Comm*. **2012**, *48*, 5328-5330; g) J. R. Brandt, X. Wang, Y. Yang, A. J. Campbell, M. J. Fuchter, *J. Am. Chem. Soc.* **2016**, *138*, 9743-9746.

[9] a) N. Ishida, T. Moriya, T. Goya, M. Murakami, M. *J. Org. Chem.* **2010**, *75*, 8709–8712; b) N. Ishida, Y. Nakanishi, T. Moriya, M. Murakami, *Chem. Lett.* **2011**, *40*, 1047-1049; c) Z. Zhao, Z. Chang, B. He, B. Chen, C. Deng, P. Lu, H. Qiu, B. Z. Tang, *Chem. Eur. J.* **2013**, *19*, 11512-11517; d) B. He, Z. Chang, Y. Jiang, B. Chen, P. Lu, H. S. Kwok, A. Qin, Z. Zhao, H. Qiu, *Dyes Pigments* **2014**, *101*, 247-253.

[10] a) R. H. Martin, J. J. Schurter, *Tetrahedron* **1972**, *28*, 1749-1758; b) C. Dallaire, I. Kolber, M. Gingras, *Org. Synth.* **2004**, *10*, 332-335; c) E. Anger, M. Srebro, N. Vanthuyne, L. Toupet, S. Rigaut, C. Roussel, J. Autschbach, J. Crassous, R. Réau, *J. Am. Chem. Soc.* **2012**, *134*, 15628-15631

[11] a) K. Mori, T. Murase, M. Fujita, *Angew. Chem. Int. Ed.* **2015**, *54*, 6847-6851; b) P. Sehnal, I. G. Stara, D. Saman, M. Tichy, J. Misek, J. Cvacka, L. Rulisek, J. Chocholousova, J. Vacek, G. Goryl, M. Szymonski, I. Cisarova, I. Stary, *PNAS* **2009**, *106*, 13169-13174.

[12] a) J. Autschbach, *Chirality* **2009**, *21*, E116-E152; b) J. Autschbach, M. Srebro, *Acc. Chem. Res.* **2014**, *47*, 2592-2602; c) M. Srebro, J. Autschbach, *J. Chem. Theory Comput.* **2012**, *8*, 245-256; d) S. Grimme, J. Antony, S. Ehrlich, H. Krieg, *J. Chem. Phys.* **2010**, *132*, 154104-154119.

[13] a) M. Srebro, N. Govind, W. de Jong, J. Autschbach, *J. Phys. Chem. A* **2011**, *115*, 10930-10949; b) M. El Sayed Moussa, M. Srebro, E. Anger, N. Vanthuyne, C. Roussel, C. Lescop, J. Autschbach, J. Crassous, *Chirality* **2013**, *25*, 455-465; c) D. H. Friese, C. Hättig, C. *Phys. Chem. Chem. Phys.* **2014,** *16,* 5942-5951.

[14] Selected examples of CPL active helicenes: a) J. E. Field, G. Muller, J. P. Riehl, D. Venkataraman, *J. Am. Chem. Soc.* **2003**, *125*, 11808-11809; b) Y. Sawada, S. Furumi, A. Takai, M. Takeuchi, K. Noguchi, K. Tanaka, *J. Am. Chem. Soc*. **2012**, *134*, 4080-4083; c) K. E. S. Phillips, T. J. Katz, S. Jockusch, A. J. Lovinger, N. J. Turro, *J. Am. Chem. Soc.* **2001**, *123*, 11899-11907; d) T. Kaseyama, S. Furumi, X. Zhang, K. Tanaka, M. Takeuchi, *Angew. Chem., Int. Ed*. **2011**, *50*, 3684-3687; e) K. Nakamura, S. Furumi, M. Takeuchi, T. Shibuya, K. Tanaka, *J. Am. Chem. Soc.* **2014**, *136*, 5555- 5558; f) N. Saleh, M. Srebro, T. Reynaldo, N. Vanthuyne, L. Toupet, V. Y. Chang, G. Muller, J. A. G. Williams, C. Roussel, J. Autschbach, J. Crassous, *Chem. Comm*. **2015**, *51*, 3754-3757; g) Y. Yamamoto, H. Sakai, J. Yuasa, Y. Araki, T. Wada, T. Sakanoue, T. Takenobu, T. Kawai, T. Hasobe, *Chem. Eur. J.* **2016**, *22*, 4263-4273; h) I. Hernandez Delgado, S. Pascal, A. Wallabregue, R. Duwald, C. Besnard, L. Guénée, C. Nançoz, E. Vauthey, R. C. Tovar, J. L. Lunkley, G. Muller, J. Lacour, *Chem. Sci.* **2016**, *7*, 4685-4693; i) H. Maeda, Y. Bando, K. Shimomura, I. Yamada, M. Naito, K. Nobusawa, H. Tsumatori, T. Kawai, *J. Am. Chem. Soc.* **2011**, *133*, 9266- 9269; j) T. Katayama, S. Nakatsuka, H. Hirai, N. Yasuda, J. Kumar, T. Kawai, T. Hatakeyama, *J. Am. Chem. Soc.* **2016**, *138*, 5210-5213.

[15] See reviews: a) H. Maeda, Y. Bando, *Pure Appl. Chem.* **2013**, *85*, 1967-1978; b) E. M. Sanchez-Carnerero, A. R. Agarrabeitia, F. Moreno, B. L. Maroto, G. Muller, M. J. Ortiz, S. de la Moya, *Chem. Eur. J.* **2015**, *21*, 13488-13500; c) J. Kumar, T. Nakashima, T. Kawai, *J. Phys. Chem. Lett.* **2015**, *6*, 3445-3452.

[16] S. Abbate, G. Longhi, F. Lebon, E. Castiglioni, S. Superchi, L. Pisani, F. Fontana, F. Torricelli, T. Caronna, C. Villani, R. Sabia, M. Tommasini, A. Lucotti, D. Mendola, A. Mele, D. A. Lightner, *J. Phys. Chem. C* **2014**, *118*, 1682-1695.

[17] a) B. Pritchard, J. Autschbach, *ChemPhysChem* **2010**, *11*, 2409-2415; b) Y. Liu, J. Cerezo, G. Mazzeo, N. Lin, X. Zhao, G. Longhi, S. Abbate, F. Santoro, *J. Chem. Theory Comput.* **2016**, *12*, 2799-2819.

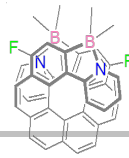

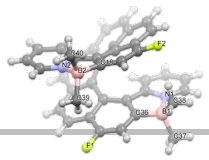

Entry for the Table of Contents (Please choose one layout)

Layout 2:

FULL PAPER

Chengshuo Shen,[a] Monika Srebro-Hooper,[b] Marion Jean,[c] Nicolas Vanthuyne,[c] Loïc Toupet,[a] J. A. Gareth Williams,[d] Alexis R. Torres,[e] Adrian J. Riives,[e] Gilles Muller,[e] Jochen Autschbach,*[f] and Jeanne Crassous*[a]*

Page No. – Page No.

Synthesis and chiroptical properties of hexa-, octa- and deca-azaborahelicenes: influence of the helicene' size and of the number of boron atoms

Cycloborylated hexa- to deca-helicenes have been prepared in enantiopure forms, along with cycloplatinated deca-helicenes. The chiroptical (electronic circular dichroism and optical rotation) and photophysical properties (unpolarized and circularly polarized luminescence) of these new chiral emissive helicenes have been studied as a function of the helicene's size and boron atoms number.